IEEE Access
Multidisciplinary ⋮ Rapid Review ⋮ Open Access Journal

Received 14 June 2024, accepted 17 August 2024, date of publication 27 August 2024, date of current version 30 September 2024.

Digital Object Identifier 10.1109/ACCESS.2024.3450539

RESEARCH ARTICLE

Applying Coherent Ising Machines for Enhancing Communication Efficiency in Large-Scale UAV-Aided Networks

TSUKUMO FUJITA[1], AOHAN LI[1,2], (Member, IEEE), QUANG VINH DO[3], TEPPEI OTSUKA[1], SEON-GEUN JEONG[4], WON-JOO HWANG[5], (Senior Member, IEEE), HIROKI TAKESUE[6], (Member, IEEE), KENSUKE INABA[6], KAZUYUKI AIHARA[7], AND MIKIO HASEGAWA[1], (Member, IEEE)

[1]Department of Electrical Engineering, Tokyo University of Science, Tokyo 125-8585, Japan
[2]Graduate School of Informatics and Engineering, The University of Electro-Communications, Tokyo 182-8585, Japan
[3]Wireless Communications Research Group, Faculty of Electrical and Electronics Engineering, Ton Duc Thang University, Ho Chi Minh City 70000, Vietnam
[4]Department of Information Convergence Engineering, Pusan National University, Yangsan-si 50612, South Korea
[5]Department of Biomedical Convergence Engineering, Pusan National University, Yangsan-si 50612, South Korea
[6]NTT Basic Research Laboratories, NTT Corporation, Tokyo 108-0075, Japan
[7]International Research Center for Neuro Intelligence, The University of Tokyo, Tokyo 113-0033, Japan

Corresponding author: Aohan Li (aohanli@ieee.org)

This work was supported in part by the Science and Technology Agency Moonshot Research and Development Program (JST Moonshot RD) under Grant JPMJMS2021 and Grant JPMJMS2216, in part by the Japan Society for the Promotion of Science KAKENHI (JSPS KAKENHI) under Grant JP20H05921, Grant JP22K14263, Grant JP23K22763, and Grant JP22H05197; in part by the Japan Agency for Medical Research and Development (AMED) under Grant JP23dm0307009; in part by the Artificial Intelligence (AI) Center, Institute of AI and Beyond, The University of Tokyo (UTokyo); in part by the 2023 Brain Korea 21 Program for Leading Universities and Students (BK21 FOUR) Program of Pusan National University; and in part by the Cross-ministerial Strategic Innovation Promotion Program (SIP), the 3rd period of SIP ''Smart energy management system'' Grant Number JPJ012207.

ABSTRACT Unmanned aerial vehicles (UAVs) are used widely in wireless communications to enhance the service experience of mobile users on the ground. This study investigates a dynamic resource management problem in a large-scale UAV-aided wireless network, where multiple UAVs operate as aerial base stations to serve ground users. To enhance communication efficiency for all users in the presence of co-channel interference, we propose the use of an Ising model-based optimization method for fast and accurate UAV-user association and resource allocation. First, we formulate the dynamic user association and resource allocation problem as a combinatorial optimization problem. Subsequently, we transform the objective function in the formulated problem into the energy function of a quadratic unconstrained binary optimization (QUBO) model and applied coherent ising machine (CIM), which has been proven to be robust for solving dense Ising problems. We evaluate our proposed method through simulations and the real CIM for optimization. Additionally, we compared our method with simulated annealing, steepest descent, and exhaustive search. Performance evaluation results indicate that our proposed method is superior in terms of computational time and data rate.

INDEX TERMS Wireless networks, multi-UAV, resource allocation, optimization methods, quantum annealing, Ising machine, D-Wave.

I. INTRODUCTION

Unmanned aerial vehicles (UAVs) are used in a wide range of communication scenarios, such as network connectivity between ground and satellite [1], maritime communication networks [2], and more broadly serving as aerial base stations [3], to enhance network coverage and performance owing to their deployment flexibility, versatility, and cost-effectiveness [4]. Taking advantage of line-of-sight (LoS) propagation, UAVs can function as aerial base stations, facilitating high spectral-efficient communications in underserved areas [5]. As a result, various UAV-based aerial platforms

The associate editor coordinating the review of this manuscript and approving it for publication was Chi-Tsun Cheng.

designed to offer wireless services have garnered significant research interest from both academic and industrial sectors [6], [7], [8], [9]. Despite these advantages, deploying UAVs for wireless communications is still challenging in practice.

Spectrum sharing is one such challenge in the design and deployment of UAV-aided networks with limited spectrum resources. Conventionally, UAV communication is implemented using unlicensed spectrum bands, such as industry and science bands [10]. Owing to the growing number of mobile devices and high-throughput applications, unlicensed spectrum is not enough to guarantee communication performance. A possible solution to this problem is sharing licensed spectrum to support high-quality connectivity for UAVs and increasing on-demand services for users [11]. However, sharing spectrum resources increases interference, especially in practical multi-UAV networks where handling co-channel interference is much more complicated than that in terrestrial systems [3], [12]. On the other hand, efficient real-time control and operation are other important aspects of UAV communications due to their lifetime and the dynamic environment [13]. As described above, the real-time combinatorial optimization, including UAV-ground User (GU) association, subchannel assignment, and transmit power of the UAV that can improve the Signal-to-Interference Ratio (SIR) to support high-quality communication in UAV networks, is extremely important.

Generally, joint optimizing UAV-GU association, subchannel assignment, and transmit power of the UAV is challenging, and evaluating such scenarios in UAV networks with a large number of users is extremely difficult. Previous related work either focused on optimizing some of these factors simultaneously but evaluated them in small-scale UAV networks [14] or targeted large-scale UAV networks by excluding complex elements such as interference between channels used for communication [15]. In addition, real-time high-speed resource allocation optimization cannot be achieved by the previous studies. To solve the problems above, in this study, we propose a high-speed resource allocation method considering the joint optimization of UAV-GU association, subchannel assignment, and transmit power for large-scale UAV networks using a coherent Ising machine (CIM).

Ising model-based optimization has been proven to be beneficial for wireless communication, which has been achieved by employing hardware-based search algorithms, such as D-Wave [16] and CIM [17]. These algorithms enable the rapid optimization of several large-scale problems. Among them, quantum annealing (QA) is a heuristic technique for solving several optimization problems that appear in a range of disciplines [16].

This study uses a CIM-based algorithm to optimize wireless resource allocation and enhance communication performance for large-scale UAV-enabled wireless networks. In particular, we investigated a joint UAV-user association, sub-channel assignment, and power control problem for downlink data transmission considering the impact of co-channel interference on network performance. The problem was first formulated as a combinatorial optimization problem, where decisions were made using binary variables, and the objective function represents the signal-to-interference ratio (SIR) of the wireless communication link. The problem was subsequently transformed into a quadratic unconstrained binary optimization (QUBO) model. We demonstrate that using a CIM-based algorithm on the resulting QUBO model can provide optimal solutions rapidly. The contribution of this study is the development of a novel framework based on Ising model-based optimization technique to find the ground energy states of the problem and provide an efficient and fast solution. Finally, we conduct extensive numerical analysis to verify the efficiency of the proposed solution in terms of computational time and data rate.

The main contributions of this paper are summarized as follows.

- We design an ultra-fast resource allocation (RA) method that considers the joint optimization of UAV-GU association, subchannel assignment, and transmit power using a CIM for large-scale UAV networks.
- To solve the formulated combinational optimization problem in UAV networks using CIM, we transform the problem into a QUBO format first. Then, we derive the interaction term and external magnetic field term used in the CIM from the transformed QUBO format.
- To confirm the effectiveness of the proposed method, we evaluate its performance and compare it with other Ising machines and heuristic algorithms. The simulation and experimental results show that the proposed method can achieve superior performance in terms of throughput for larger-scale problems compared to other Ising machines. Additionally, the proposed method also shows superior performance in terms of throughput and execution time compared to other heuristic methods.

The rest of this paper is organized as follows. Section II describes the related work on the UAV network and Ising machine. Section III introduces the system model and formulates the problem. Section IV introduces the principle of CIM for solving optimization problems. Section V presents the conversion to the QUBO model and the approach for CIM required to solve the optimization problem introduced in Section III. Section VI shows the performance evaluation in various scale UAV networks. Section VII discusses the results and future work. Section VIII concludes this study.

II. RELATED WORK

In this section, we review recent work. First, we present the related work on resource allocation for UAV networks. Then, we introduce the related work on quantum and optical Ising machines, including CIM and D-Wave. Next, we explain the related work on resource allocation using Ising machines in wireless communications. Finally, we summarize the drawbacks of the related work and the motivation of this

TABLE 1. Comparison of the existing studies and this paper.

Refs.	Optimization methods	Variables being optimized	Scalability	Processing computation time	Hardware for implementation
[14]	Deep reinforcement learning	UAV-user association, Power allocation	12 users, 4 UAVs	5.99s	CPU
[15]	Deep reinforcement learning	UAV trajectory Power allocation	50 users, 9 UAVs	-	CPU or GPU
[21]	Heuristic algorithm	User-BS association UAV trajectory Interference Reflect Surface (IRS) beamforming angle	4 users, 1 UAV 100 time slots	-	CPU
[31]	D-wave	IRS-User association, Time slot allocation	6 users, 3 IRS, 10 time slots	3s	D-wave Hybrid solver
This paper	CIM	UAV-User association, Channel allocation, Power allocation	40 users, 15 UAVs, 12 channels	22ms [29]	Ising machine

paper. Moreover, to clarify the motivation of this paper, we give a table to compare the related work and this paper in terms of variables being optimized, scalability, process computing time, and hardware for implementation.

A. RA FOR UAV NETWORK

The optimization problems in many previous studies related to UAV networks focus on network-performance optimization, targeting the optimization of UAV trajectories, configurations, communicating users, UAV transmission power, and other factors. Additionally, factors such as interference between channels in communication also need to be considered. Generally, optimizing these elements together becomes highly complex and challenging. Several recent studies on heuristic solutions conducted optimization with a narrowed focus, e.g., energy saving [18], time and power optimization [19], offloading and computing [2], UAV trajectory optimization [20], [21], placement and transmit power allocation [22], and secure communication [23]. In addition, most existing studies considered small-scale networks with only a few UAVs and a small number of users [2], [20], [21], [22]. However, optimizing multiple elements simultaneously and rapidly in a practical large-scale UAV network is necessary for real applications.

Some recent studies have employed Deep Reinforcement Learning (DRL) to optimize multiple elements for UAV networks simultaneously. In [14], channel interference is considered when allocating resources in multiple UAV networks with dynamic users. Reference [15] studies trajectory design and resource allocation in multiple UAV networks. In [24], the selection of service UAVs and transmission power of the UAV optimization problem is investigated for improving video quality. In [25], the jointly optimal problem of UAV-user pairing and UAV placement is studied to minimize the average task delay of the task offloading in MEC networks. However, the large training time of the neural network model in DRL is needed to adapt to dynamic, varied environments, which may be challenging when applied to the resource allocation problems in the UAV networks with real-time applications.

B. QUANTUM AND OPTICAL ISING MACHINES FOR RA

Quantum machines based on the dynamics of physical systems have been utilized to solve optimization problems in recent years since they can quickly solve NP-hard problems. D-Wave and CIM are the two well-known physical-systems-based machines. D-wave [16] is a commercially available QA machine based on superconducting quantum bits, and CIM [17], [26], [27], [28], also known as the optical Ising machine, is a laser network-based optimizer that can provide approximate solutions to combinatorial optimization problems with computing speed that is in the order of milliseconds. Several NP-complete and NP-hard problems can be converted to ground-state search problems in the Ising model [29]. CIM and D-Wave QA can rapidly obtain states close to the ground state of the Ising Hamiltonian, which represents optimal solutions to optimization problems. The difference between D-Wave QA and CIM is that in D-Wave QA, the magnetic spin network is reproduced in a chimera or Pegasus topology with sparse connections, while in CIM, the Ising network of optical pulses generated by a laser oscillator is fully coupled [26], [27]. Honjo et al. demonstrated that 100,000 fully coupled spins can be implemented in CIM [28]. Numerous complex optimization problems are described as larger, massively connected models with dense graph structures. For these problems, CIM has been demonstrated to be faster than D-Wave QA [30]. This may be attributed to the fact that D-Wave QA has a sparse graph structure that requires more logical qubits to represent a fully connected graph, making complex optimization problems difficult to solve [30]. These physical-systems-based machines have already been studied for resource allocation optimization problems in wireless communication. In [31], D-Wave QA is used to solve the scheduling optimization problem of the Intelligent Reflecting Surface (IRS) in wireless communication systems. In [32], [33], [34], and [35], the resource allocation optimization problems in NOMA and WLAN systems are studied using CIM.

C. MOTIVATION OF THIS PAPER

As described above, the existing work for the resource allocation problems in the large-scale UAV network is

challenging to adapt to dynamic, varied environments with real-time applications. Fortunately, CIM can solve large-scale optimization problems in millisecond order. Hence, in this paper, we use CIM to solve the complex resource allocation joint optimization problem, including UAV-GU association, subchannel assignment, and transmit power allocation in large-scale UAV networks. To make the motivation of this paper more straightforward, we compare several existing studies with our system in terms of the optimization method, variables being optimized, scalability, processing computation time, and hardware for implementation in Table 1.

III. SYSTEM MODEL AND PROBLEM FORMULATION

A. SYSTEM MODEL

We consider a large-scale UAV-enabled wireless network consisting of a macro base station (MBS) and M single-antenna UAVs operating as aerial base stations at a constant altitude. Fig.1 shows the system model in UAV networks. N ground users (GUs) are randomly distributed within the circular geographical area of radius r_c of the MBS. The MBS is equipped with a hardware-based CIM, which is responsible for communicating the optimal user connection, channel, and power level selection to the UAVs. We denote the sets of UAVs and users as $\mathcal{M} = \{1, \ldots, M\}$ and $\mathcal{N} = \{1, \ldots, N\}$, respectively. The total system bandwidth is divided into K orthogonal subchannels, denoted by $\mathcal{K} = \{1, \ldots, K\}$. Notably, the subchannels allocated to the UAVs may overlap with each other. We assume the MBS is the network controller and that the UAVs can exchange information with the controller via perfect backhaul connections. Furthermore, the controller makes decisions about UAV-user association, subchannel assignment, and power control for downlink data transmissions.

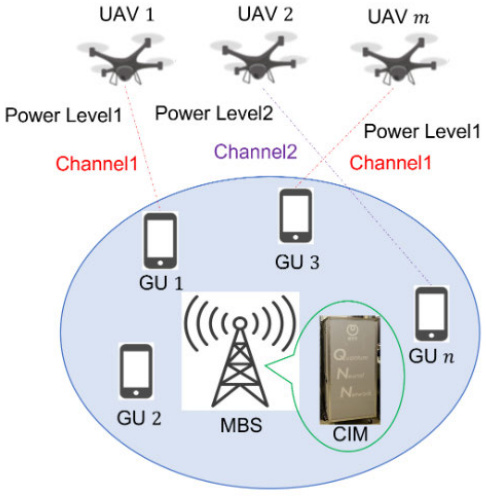

FIGURE 1. System model in UAV networks.

The locations of UAV $m \in \mathcal{M}$ and GU $n \in \mathcal{N}$ in a three-dimensional space are denoted by $\boldsymbol{q}_m^{UAV} = (x_m, y_m, H)$ and $\boldsymbol{q}_n^{GU} = (x_n, y_n, 0)$, respectively, where H is the hovering altitude of the UAV. Similar to a previous study [36], this study considered a probabilistic air-to-ground path-loss model, in which the communication channels between the UAVs and the GUs can be modeled as either line-of-sight (LoS) or non-line-of-sight (NLoS) links. Particularly, the probability that the channel between UAV m and GU n is LoS, denoted as $\rho_{m,n}^{LoS}$, is given by [37]:

$$\rho_{m,n}^{LoS} = \frac{1}{1 + ae^{-b\left(\frac{180}{\pi}\arcsin\left(\frac{H}{d_{m,n}}\right) - a\right)}}, \tag{1}$$

where a and b are the environment-dependent parameters, and $d_{m,n} = \sqrt{\|\boldsymbol{q}_m^{UAV} - \boldsymbol{q}_n^{GU}\|^2}$ is the distance between them. Hence, the probabilistic path loss is given by [36]:

$$g_{m,n} = \left(\rho_{m,n}^{LoS} + \left(1 - \rho_{m,n}^{LoS}\right)\eta\right) g_{m,n}^{LoS}, \tag{2}$$

where $g_{m,n}^{LoS} = g_0 {d_{m,n}}^{-\epsilon_0}$ represents the free-space channel gain, g_0 is the channel gain at the reference distance $d_0 = 1$ m, ϵ_0 is the path-loss exponent, and η is the additional signal attenuation factor due to NLoS condition.

We denote $\alpha_{m,n} \in \{0, 1\}$ as the association variable between UAV m and GU n, i.e., if GU n is associated with UAV m, $\alpha_{m,n} = 1$; otherwise, $\alpha_{m,n} = 0$. In this study, we assume that each UAV can only associate with one GU at a time. Thus, the following constraint must hold

$$\sum_{n \in \mathcal{N}} \alpha_{m,n} \leq 1, \ \forall m \in \mathcal{M}, \tag{3}$$

Similarly, we denote $\beta_m^k \in \{0, 1\}$ as the subchannel assignment variable, i.e., if channel k is allocated to UAV m, $\beta_m^k = 1$, otherwise, $\beta_m^k = 0$. This gives us:

$$\sum_{k \in \mathcal{K}} \beta_m^k \leq 1, \ \forall m \in \mathcal{M}, \tag{4}$$

which indicates that each UAV can only occupy a single subchannel at a time.

Consequently, the SIR for the communication link between UAV m and GU n on subchannel k is given as:

$$\gamma_{m,n}^k = \frac{g_{m,n}\alpha_{m,n}\beta_m^k P_m}{I_{m,n}^k}, \tag{5}$$

where P_m denotes the transmit power of UAV m, and $I_{m,n}^k$ is the co-channel interference at UAV m caused by other UAVs operating on subchannel k, which is given as:

$$I_{m,n}^k = \sum\nolimits_{m' \in \mathcal{M}, m' \neq m} g_{m',n}\beta_{m'}^k P_{m'}, \tag{6}$$

where $P_{m'}$ denote the transmit power of UAV m'. Thus, the SIR for UAV m, denoted as S_m, can be calculated as follows:

$$S_m = \sum_{n \in \mathcal{N}} \sum_{k \in \mathcal{K}} \gamma_{m,n}^k, \ \forall m \in \mathcal{M}, \tag{7}$$

In a network with multiple UAVs, the co-channel interference might be large enough to deteriorate the communication links between a UAV and its associated user. Hence, it is important to make efficient user association, subchannel assignment, and power-control decisions. Hence, our objective is maximizing the SIR. Moreover, the data rate can be used to

evaluate the performance of the UAV networks, which is obtained using Shannon's theorem as follows:

$$R = B\log(1 + SINR), \tag{8}$$

where SINR is the signal-to-interference and noise power ratio (SINR), which can be calculated as follows:

$$SINR = \frac{\sum_{m\in\mathcal{M}}\sum_{n\in\mathcal{N}}\sum_{k\in\mathcal{K}} g_{m,n}\alpha_{m,n}\beta_m^k P_m}{\sum_{m\in\mathcal{M}}\sum_{n\in\mathcal{N}}\sum_{k\in\mathcal{K}} I_{m,n}^k + k_B TB}. \tag{9}$$

Here, k_B represents the Boltzmann constant, T represents the temperature, and B represents the bandwidth of the network.

B. PROBLEM FORMULATION

We aim to maximize the communication efficiency in terms of average system SIR by controlling UAV-GU association, subchannel assignment, and transmit power of the UAVs. In this study, discrete transmit power control is adopted in UAVs. More specifically, the transmit power values by a UAV to communicate with its associated user can be selected in a list $\{P_1, P_2, \ldots, P_L\}$, where $P_1 \le P_2 \le \cdots \le P_L$. Let $p_m^l \in \{0, 1\}$, $l \in \mathcal{L} = \{1, \ldots, L\}$ denote the power control variable, i.e., if UAV m selects transmit power at level l, $p_m^l = 1$; otherwise, $p_m^l = 0$. Note that only one power level can be selected by UAV m at a time. Thus, we formulated as:

$$\sum_{l\in\mathcal{L}} p_m^l \le 1, \ \forall m \in \mathcal{M}, \tag{10}$$

Therefore, the SIR for UAV m in (7) can be recast as:

$$S_m = \sum_{n\in\mathcal{N}}\sum_{k\in\mathcal{K}}\sum_{l\in\mathcal{L}} \gamma_{m,n}^{k,l}, \ \forall m \in \mathcal{M}, \tag{11}$$

Consequently, the SIR maximization problem can be formulated as follows:

$$\begin{aligned}
&\max_{\boldsymbol{\alpha},\boldsymbol{\beta},\boldsymbol{P}} \overline{S} = \sum_{m\in\mathcal{M}} S_m, \\
&s.t. \ \sum\nolimits_{n\in\mathcal{N}} \alpha_{m,n} \le 1, \ \forall m \in \mathcal{M}, \\
&\quad \sum\nolimits_{k\in\mathcal{K}} \beta_m^k \le 1, \ \forall m \in \mathcal{M}, \\
&\quad \sum\nolimits_{l\in\mathcal{L}} p_m^l \le 1, \ \forall m \in \mathcal{M}, \\
&\quad \alpha_{m,n} \in \{0, 1\}, \ \beta_n^k \in \{0, 1\}, \ p_m^l \in \{0, 1\},
\end{aligned} \tag{12}$$

where $\boldsymbol{\alpha} = \{\alpha_{m,n}\}_{M\times N}$ and $\boldsymbol{\beta} = \{\beta_m^k\}_{K\times M}$ represent the user association and subchannel assignment matrices, and $\boldsymbol{P} = \{p_m^l\}_{L\times M}$ denotes the transmit power control matrix.

IV. COHERENT ISING MACHINE

A. ISING HAMILTONIAN

CIM is an Ising-type machine that can artificially reproduce the Ising model, a physical model of magnetic spin. The Ising model consists of two states of magnetic spins: upward and downward. The spins are mutually coupled and are affected by interactions from other spins as well as from external magnetic fields. We consider an Ising model with a four-dimensional structure of $M \times N \times K \times L$. Here, the Ising Hamiltonian, which is the energy function of the Ising model, is expressed as follows.

$$\begin{aligned}
E(\sigma) = -\frac{1}{2}\sum_{i=1}^{\mathcal{M}}\sum_{j=1}^{\mathcal{N}}\sum_{k=1}^{\mathcal{K}}\sum_{l=1}^{\mathcal{L}}\sum_{i'=1}^{\mathcal{M}}\sum_{j'=1}^{\mathcal{N}}\sum_{k'=1}^{\mathcal{K}}\sum_{l'=1}^{\mathcal{L}} \\
J_{ijkl,i'j'k'l'}\sigma_{ijkl}\sigma_{i'j'k'l'} \\
+\sum_{i=1}^{\mathcal{M}}\sum_{j=1}^{\mathcal{N}}\sum_{k=1}^{\mathcal{K}}\sum_{l=1}^{\mathcal{L}} \lambda_{ijkl}\sigma_{ijkl},
\end{aligned} \tag{13}$$

where $\sigma_{ijkl} \in \{-1, +1\}$ is the spin direction of the (i, j, k, l)-th spin, $J_{ijkl,i'j'k'l'}$ is the strength of the interaction between the (i, j, k, l)-th spin and the (i', j', k', l')-th spin, λ_{ijkl} is the strength of the external magnetic field to the (i, j, k, l)-th spin. CIM is a machine that can obtain the ground state of this Ising Hamiltonian at high speeds. In other words, by setting $J_{ijkl,i'j'k'l'}$ and λ_{ijkl} corresponding to the optimal solution of the optimization problem to the maximum values in Eq.(12) and using CIM, the optimal solution of the target optimization problem can be approximated and obtained rapidly.

B. MEASUREMENT FEEDBACK COHERENT ISING MACHINE

Initial CIM was laser networks consisting of one primary laser and multiple secondary lasers [38]. Recently, measurement feedback CIM has been proposed to solve large-scale problems, where the coupling matrix can be arbitrarily designed [26], [27]. In measurement feedback CIM, the parameters of the Ising model, i.e., $J_{ijkl,i'j'k'l'}$ and λ_{ijkl}, are preconfigured in a Field Programmable Gate Array (FPGA) module. The FPGA module calculates the feedback values using these set parameters and feeds them back to the original pulse. Moreover, the CIM also requires proper setting parameters for input light intensity, feedback light intensity adjustment, and pump schedule. Thus, the interaction between the spins can be reproduced programmatically, making it possible to fully connect the spins. Furthermore, the phase of the degenerate optical parametric oscillator (DOPO) pulse orbiting on the optical fiber represents the Ising spin σ_{ijkl}. In [28], it is demonstrated that 100,000 DOPO pulses can be realized on a 5-km polarization-maintaining optical fiber, reaching the reference score for the 100,000-node MAX-CUT problem within 593 μs.

V. CIM-BASED SOLUTION

This section describes the solution of the optimization problem by using Ising model-based optimization. First, we reformulate the problem as an objective function in the QUBO model. Subsequently, we apply a CIM-based technique to determine the low energy states of the model by deriving the quadratic coefficients and the linear coefficients.

A. PROBLEM TRANSFORMATION

1) TRANSFORMATION OF THE OBJECTIVE FUNCTION

Firstly, the SIR for the communication link between UAV m and GU n on subchannel k using power level l, i.e., $\gamma_{m,n}^{k,l}$

shown in Eq. (5) can be transformed into:

$$\gamma_{m,n}^{k,l} = \frac{\alpha_{m,n}\beta_m^k p_m^l g_{m,n} P_l}{\sum_{m'\in\mathcal{M},m'\neq m}\sum_{n'\in\mathcal{N}}\sum_{l'\in\mathcal{L}}\alpha_{m,n}\alpha_{m',n'}\beta_m^k\beta_{m'}^k p_{m'}^{l'} g_{m',n} P_{l'}}, \tag{14}$$

Subsequently, the objective function in Eq. (12) can be transformed into:

$$\max_{\boldsymbol{\alpha},\boldsymbol{\beta},\boldsymbol{P}} \sum_{m\in\mathcal{M}}\sum_{n\in\mathcal{N}}\sum_{k\in\mathcal{K}}\sum_{l\in\mathcal{L}}\gamma_{m,n}^{k,l}. \tag{15}$$

We denote X_{mnkl} as the neuron. $X_{mnkl} = 1$ if UAV m associate with GU n using channel k with power level l, i.e.,

$$X_{mnkl} = \begin{cases} 1, & \text{if UAV } m \text{ associate with GU } n \\ & \text{using channel } k \text{ with power level } l. \\ 0, & \text{otherwise.} \end{cases} \tag{16}$$

To solve optimization problems using the Ising model-based method, it is necessary to transform the equation into a form similar to the one shown in Eq. (13) and derive $J_{ijkl,i'j'k'l'}$ and λ_{ijkl}. Subsequently, the objective function shown in Eq. (15) can be transformed into:

$$\max_{\boldsymbol{X}} \sum_{m\in\mathcal{M}}\sum_{n\in\mathcal{N}}\sum_{k\in\mathcal{K}}\sum_{l\in\mathcal{L}} \frac{X_{mnkl} g_{m,n} P_l}{\sum_{m'\in\mathcal{M},m'\neq m}\sum_{n'\in\mathcal{N}}\sum_{l'\in\mathcal{L}} X_{mnkl} X_{m'n'kl'} g_{m',n} P_{l'}} + \sum_{m'\in\mathcal{M}}\sum_{n'\in\mathcal{N}}\sum_{k'\in\mathcal{K}}\sum_{l'\in\mathcal{L}} \frac{X_{m'n'k'l'} g_{m',n'} P_{l'}}{\sum_{m\in\mathcal{M},m\neq m'}\sum_{n\in\mathcal{N}}\sum_{l\in\mathcal{L}} X_{m'n'k'l'} X_{mnk'l} g_{m,n'} P_l}. \tag{17}$$

By taking the reciprocal, the above equation can be transformed into:

$$\min_{\boldsymbol{X}} \sum_{m\in\mathcal{M}}\sum_{n\in\mathcal{N}}\sum_{k\in\mathcal{K}}\sum_{l\in\mathcal{L}}\sum_{m'\in\mathcal{M},m'\neq m}\sum_{n'\in\mathcal{N}}\sum_{l'\in\mathcal{L}} \left(\frac{g_{m',n} P_{l'}}{g_{m,n} P_l} + \frac{g_{m,n'} P_l}{g_{m',n'} P_{l'}}\right) X_{mnkl} X_{m'n'kl'}. \tag{18}$$

By introducing Kronecker delta $\delta_{mm'}$ and $\delta_{kk'}$, Eq. (18) can be expressed as:

$$\min_{\boldsymbol{X}} \sum_{m\in\mathcal{M}}\sum_{n\in\mathcal{N}}\sum_{k\in\mathcal{K}}\sum_{l\in\mathcal{L}}\sum_{m'\in\mathcal{M}}\sum_{n'\in\mathcal{N}}\sum_{k'\in\mathcal{K}}\sum_{l'\in\mathcal{L}} \left(\frac{g_{m',n} P_{l'}}{g_{m,n} P_l} + \frac{g_{m,n'} P_l}{g_{m',n'} P_{l'}}\right) (1-\delta_{mm'})\,\delta_{kk'} X_{mnkl} X_{m'n'k'l'}. \tag{19}$$

2) TRANSFORMATION OF THE CONSTRAINT

The constraints can be expressed as:

$$E_2 = \sum_{m=1}^{\mathcal{M}} \left(\sum_{n=1}^{\mathcal{N}}\sum_{k=1}^{\mathcal{K}}\sum_{l=1}^{\mathcal{L}} X_{mnkl} - 1\right)^2$$

$$= \sum_{m=1}^{\mathcal{M}} \left(\left(\sum_{n=1}^{\mathcal{N}}\sum_{k=1}^{\mathcal{K}}\sum_{l=1}^{\mathcal{L}} X_{mnkl}\right)^2 - 2\left(\sum_{n=1}^{\mathcal{N}}\sum_{k=1}^{\mathcal{K}}\sum_{l=1}^{\mathcal{L}} X_{mnkl}\right) + 1 \right)$$

$$= \sum_{m=1}^{\mathcal{M}}\sum_{n=1}^{\mathcal{N}}\sum_{k=1}^{\mathcal{K}}\sum_{l=1}^{\mathcal{L}}\sum_{n'=1}^{\mathcal{N}}\sum_{k'=1}^{\mathcal{K}}\sum_{l'=1}^{\mathcal{L}} X_{mnkl} X_{mn'k'l'} - 2\sum_{m=1}^{\mathcal{M}}\sum_{n=1}^{\mathcal{N}}\sum_{k=1}^{\mathcal{K}}\sum_{l=1}^{\mathcal{L}} X_{mnkl} + M. \tag{20}$$

Here, when $n = n'$, $k = k'$ and $l = l'$, represent $X_{mnkl} = X_{mn'k'l'}$. However, the multiplication of the same spins must be 0 to compare with Ising Hamiltonian. That is, when $n = n'$, $k = k'$ and $l = l'$, $X_{mnkl} X_{mn'k'l'} = 0$. Hence, Eq. (20) can be expressed as:

$$\begin{aligned} E_2 &= \sum_{m=1}^{\mathcal{M}}\sum_{n=1}^{\mathcal{N}}\sum_{k=1}^{\mathcal{K}}\sum_{l=1}^{\mathcal{L}}\sum_{n'=1}^{\mathcal{N}}\sum_{k'=1}^{\mathcal{K}}\sum_{l'=1}^{\mathcal{L}} (1-\delta_{nn'}\delta_{kk'}\delta_{ll'})\, X_{mnkl} X_{mn'k'l'} \\ &\quad + \sum_{m=1}^{\mathcal{M}}\sum_{n=1}^{\mathcal{N}}\sum_{k=1}^{\mathcal{K}}\sum_{l=1}^{\mathcal{L}}\sum_{n'=1}^{\mathcal{N}}\sum_{k'=1}^{\mathcal{K}}\sum_{l'=1}^{\mathcal{L}} \delta_{nn'}\delta_{kk'}\delta_{ll'} X_{mnkl} X_{mn'k'l'} \\ &\quad - 2\sum_{m=1}^{\mathcal{M}}\sum_{n=1}^{\mathcal{N}}\sum_{k=1}^{\mathcal{K}}\sum_{l=1}^{\mathcal{L}} X_{mnkl} + M \\ &= \sum_{m=1}^{\mathcal{M}}\sum_{n=1}^{\mathcal{N}}\sum_{k=1}^{\mathcal{K}}\sum_{l=1}^{\mathcal{L}}\sum_{n'=1}^{\mathcal{N}}\sum_{k'=1}^{\mathcal{K}}\sum_{l'=1}^{\mathcal{L}} (1-\delta_{nn'}\delta_{kk'}\delta_{ll'})\, X_{mnkl} X_{mn'k'l'} + \sum_{m=1}^{\mathcal{M}}\sum_{n=1}^{\mathcal{N}}\sum_{k=1}^{\mathcal{K}}\sum_{l=1}^{\mathcal{L}} X_{mnkl} \\ &\quad - 2\sum_{m=1}^{\mathcal{M}}\sum_{n=1}^{\mathcal{N}}\sum_{k=1}^{\mathcal{K}}\sum_{l=1}^{\mathcal{L}} X_{mnkl} + M \\ &= \sum_{m=1}^{\mathcal{M}}\sum_{n=1}^{\mathcal{N}}\sum_{k=1}^{\mathcal{K}}\sum_{l=1}^{\mathcal{L}}\sum_{n'=1}^{\mathcal{N}}\sum_{k'=1}^{\mathcal{K}}\sum_{l'=1}^{\mathcal{L}} (1-\delta_{nn'}\delta_{kk'}\delta_{ll'})\, X_{mnkl} X_{mn'k'l'} \\ &\quad - \sum_{m=1}^{\mathcal{M}}\sum_{n=1}^{\mathcal{N}}\sum_{k=1}^{\mathcal{K}}\sum_{l=1}^{\mathcal{L}} X_{mnkl} + M. \end{aligned} \tag{21}$$

By introducing Kronecker delta $\delta_{mm'}$, Eq. (21) can be expressed as:

$$E_2 = \sum_{m=1}^{\mathcal{M}}\sum_{n=1}^{\mathcal{N}}\sum_{k=1}^{\mathcal{K}}\sum_{l=1}^{\mathcal{L}}\sum_{m'=1}^{\mathcal{M}}\sum_{n'=1}^{\mathcal{N}}\sum_{k'=1}^{\mathcal{K}}\sum_{l'=1}^{\mathcal{L}} \delta_{mm'}\,(1-\delta_{nn'}\delta_{kk'}\delta_{ll'})\, X_{mnkl} X_{m'n'k'l'} - \sum_{m=1}^{\mathcal{M}}\sum_{n=1}^{\mathcal{N}}\sum_{k=1}^{\mathcal{K}}\sum_{l=1}^{\mathcal{L}} X_{mnkl} + M. \tag{22}$$

From the above, Eq. (12) can be transformed into the following QUBO problem:

$$\min_{\boldsymbol{X}} AE_1 + BE_2,$$

$$E_1 = \sum_{m\in\mathcal{M}}\sum_{n\in\mathcal{N}}\sum_{k\in\mathcal{K}}\sum_{l\in\mathcal{L}}\sum_{m'\in\mathcal{M}}\sum_{n'\in\mathcal{N}}\sum_{k'\in\mathcal{K}}\sum_{l'\in\mathcal{L}} \left(\frac{g_{m',n}P_{l'}}{g_{m,n}P_l} + \frac{g_{m,n'}P_l}{g_{m',n'}P_{l'}}\right)(1-\delta_{mm'})\,\delta_{kk'}X_{mnkl}X_{m'n'k'l'},$$

$$E_2 = \sum_{m=1}^{\mathcal{M}}\sum_{n=1}^{\mathcal{N}}\sum_{k=1}^{\mathcal{K}}\sum_{l=1}^{\mathcal{L}}\sum_{m'=1}^{\mathcal{M}}\sum_{n'=1}^{\mathcal{N}}\sum_{k'=1}^{\mathcal{K}}\sum_{l'=1}^{\mathcal{L}} \delta_{mm'}\,(1-\delta_{nn'}\delta_{kk'}\delta_{ll'})\,X_{mnkl}X_{m'n'k'l'} - \sum_{m=1}^{\mathcal{M}}\sum_{n=1}^{\mathcal{N}}\sum_{k=1}^{\mathcal{K}}\sum_{l=1}^{\mathcal{L}} X_{mnkl} + M. \tag{23}$$

B. CIM-BASED APPROACH

We consider a neural network with a four-dimensional structure of $M \times N \times K \times L$; the mutually connected network has the following energy structure:

$$E(x) = -\frac{1}{2}\sum_{i=1}^{\mathcal{M}}\sum_{j=1}^{\mathcal{N}}\sum_{k=1}^{\mathcal{K}}\sum_{l=1}^{\mathcal{L}}\sum_{i'=1}^{\mathcal{M}}\sum_{j'=1}^{\mathcal{N}}\sum_{k'=1}^{\mathcal{K}}\sum_{l'=1}^{\mathcal{L}} w_{ijkl,i'j'k'l'}x_{ijkl}x_{i'j'k'l'} + \sum_{i=1}^{\mathcal{M}}\sum_{j=1}^{\mathcal{N}}\sum_{k=1}^{\mathcal{K}}\sum_{l=1}^{\mathcal{L}}\theta_{ijkl}x_{ijkl}, \tag{24}$$

where $x_{ijkl} \in \{0, 1\}$ is the state of the (i, j, k, l)-th neuron, $w_{ijkl,i'j'k'l'}$ is the coupling weight between the (i, j, k, l)-th and (i', j', k', l')-th neurons, and θ_{ijkl} is the firing threshold of the (i, j, k, l)-th neuron. From the similarity of the energy structure of the Ising Hamiltonian and that of the mutually connected neural network, i.e., Eq. (13), the parameters of the CIM, $J_{ijkl,i'j'k'l'}$ and λ_{ijkl}, can be derived using the parameters (i.e., $w_{ijkl,i'j'k'l'}$ and θ_{ijkl}) of the mutually coupled neural network. Hence, by comparing Eq. (23) and Eq.(24),the coupling weight $w_{ijkl,i'j'k'l'}$ and the threshold θ_{ijkl} are obtained as follows:

$$w^1_{ijkl,i'j'k'l'} = -2\,(1-\delta_{ii'})\,\delta_{kk'}\left(\frac{g_{i',j}P_{l'}}{g_{i,j}P_l} + \frac{g_{i,j'}P_l}{g_{i',j'}P_{l'}}\right), \tag{25}$$

$$\theta^1_{ijkl} = 0, \tag{26}$$

$$w^2_{ijkl,i'j'k'l'} = -2\delta_{ii'}\left(1-\delta_{jj'}\delta_{kk'}\delta_{ll'}\right), \tag{27}$$

$$\theta^2_{ijkl} = -1, \tag{28}$$

$$\begin{aligned} w_{ijkl,i'j'k'l'} &= Aw^1_{ijkl,i'j'k'l'} + Bw^2_{ijkl,i'j'k'l'} \\ &= -2A\,(1-\delta_{ii'})\,\delta_{kk'}\left(\frac{g_{i',j}P_{l'}}{g_{i,j}P_l} + \frac{g_{i,j'}P_l}{g_{i',j'}P_{l'}}\right) \\ &\quad - 2B\delta_{ii'}\left(1-\delta_{jj'}\delta_{kk'}\delta_{ll'}\right), \end{aligned} \tag{29}$$

$$\begin{aligned} \theta_{ijkl} &= A\theta^1_{ijkl} + B\theta^2_{ijkl} \\ &= -B. \end{aligned} \tag{30}$$

Since $w_{ijkl,i'j'k'l'}$ and θ_{ijkl} correspond to $x_{ijkl} \in \{0, 1\}$, while $J_{ijkl,i'j'k'l'}$ and λ_{ijkl} correspond to $\sigma_{ijkl} \in \{-1, +1\}$ in the Ising model, we transform as follows:

$$\sigma_{ijkl} = 2x_{ijkl} - 1. \tag{31}$$

The connecting weights $J_{ijkl,i'j'k'l'}$ of the Ising model and the external magnetic field λ_{ijkl} can be derived using Eqs.(29), (30), and (31), which are expressed as follows:

$$J_{ijkl,i'j'k'l'} = \frac{w_{ijkl,i'j'k'l'}}{2}, \tag{32}$$

$$\lambda_{ijkl} = \theta_{ijkl} - \frac{\sum_{i'=1}^{\mathcal{M}}\sum_{j'=1}^{\mathcal{N}}\sum_{k'=1}^{\mathcal{K}}\sum_{l'=1}^{\mathcal{L}} w_{ijkl,i'j'k'l'}}{2}. \tag{33}$$

The detailed derivation process can be found in [32].

VI. PERFORMANCE EVALUATION

In this section, we evaluate the performance of our proposed CIM-based algorithm in UAV networks. We utilize the data rate R as network performance metric, a common metric for evaluating networks. In the following, the total data rate of the UAV network system and the processing time of the proposed method are evaluated and compared. Specifically, we compare it with Simulated Annealing (SA), which is a meta-heuristic optimization method, Steepest Descent (SD), D-Wave, and Exhaustive Search (ES). Among these comparative methods, SA and ES are techniques that have been used in simulation evaluations for performance comparisons with CIM in previous studies [32]. Additionally, since SD is an algorithm similar to ground state search in the Ising model [39] while the D-Wave [31] is another type of Ising machine, we utilized the SD algorithm and D-Wave as a comparison method in the performance evaluation. Next, we provide a detailed description of each method.

Herein, we used the following simulation model of the CIM to evaluate the proposed method.

$$\frac{dc_{ijkl}}{dt} = \left(-1 + p - c^2_{ijkl} - s^2_{ijkl}\right)c_{ijkl} + \sum_{i'=1}^{\mathcal{M}}\sum_{j'=1}^{\mathcal{N}}\sum_{k'=1}^{\mathcal{K}}\sum_{l'=1}^{\mathcal{L}} J_{ijkl,i'j'k'l'}c_{i'j'k'l'} - \lambda_{ijkl}, \tag{34}$$

$$\frac{ds_{ijkl}}{dt} = \left(-1 - p - c^2_{ijkl} - s^2_{ijkl}\right)s_{ijkl} + \sum_{i'=1}^{\mathcal{M}}\sum_{j'=1}^{\mathcal{N}}\sum_{k'=1}^{\mathcal{K}}\sum_{l'=1}^{\mathcal{L}} J_{ijkl,i'j'k'l'}s_{i'j'k'l'} - \lambda_{ijkl}, \tag{35}$$

where c_{ijkl} and s_{ijkl} are the in-phase and quadrature phase amplitudes of the (i, j, k, l)-th optical pulse, respectively, and p is the pump pulse, used to amplify c_{ijkl}. By simulating while gradually increasing p, we can obtain the in-phase and quadrature components of the DOPO pulse. As described in Section III, the measurement feedback CIM reproduces the Ising spin using the amplitude of the DOPO pulse circulating on a long optical fiber. In this case, we used a simulation model to reproduce the behavior of the CIM and obtain a combination of spins that minimizes the Hamiltonian. The

Ising spin σ_{ijkl} is expressed as the magnitude of c_{ijkl}, where $\sigma_{ijkl} = -1$, if $c_{ijkl} < 0$ and $\sigma_{ijkl} = +1$, if $c_{ijkl} > 0$.

We compare the CIM-based with the SA, SD, and ES methods. The Boltzmann machine model [40] was also used as the computational model for SA. A Boltzmann machine is an interconnected neural network incorporating statistical behavior. Specifically, the model is a sigmoid function that introduces a temperature T into the output function, and the values of neurons $X \in \{0, 1\}$ change stochastically with temperature T. In the simulation, the initial temperature of SA and the rate of decrease of temperature per iteration were set as parameters and measured with parameter tuning.

SD is a numerical analysis algorithm for finding the minimum value. It moves in the direction of the steepest descent from the initial state to the direction where the objective function becomes the smallest, and searches for the minimum value of the function until it converges [39].

ES is a brute-force search algorithm that explores all possible combinations to find the optimal solution. Although this algorithm guarantees an optimal solution by searching all possibilities, it is impractical for a large search space in a realistic time.

We perform our evaluation on three scales of UAV networks. Firstly, a small-scale UAV network where the D-wave can solve the scale of the problem. The purpose of this experiment evaluation is to compare the performance of Ising machines. Secondly, a middle-scale UAV network where the ES can operate in a realistic time. The purpose of this simulation evaluation is to confirm the proposed method reaching the optimal solution solved by ES. Finally, a large UAV network was used to verify the performance of the proposed and comparative methods. ES was excluded from the comparison methods for large-scale networks because it does not provide solutions in a realistic time. This is because the scale of networks becomes too large for ES to solve in a realistic time since ES is a brute-force search algorithm.

Table 2 shows the parameter settings in UAV networks. The simulation parameters in this table are common to small and large UAV networks. The UAVs and GUs were randomly distributed in the service area of the MBS. In this simulation, we considered UAV network systems in which the MBS was placed at the center of a circular cell with a radius of 1000 m.

TABLE 2. Parameters settings in UAV networks.

Parameter	Value
Service area radius, r_c	1000 m
Environment-dependent parameters a and b	$a = 10, b = 0.6$
Free-space channel gain g_0	-30 dB
Path-loss exponent ϵ_0	2
Additional signal attenuation factor η	0.2
UAVs' altitude H	100 m
Bandwidth of the entire network B	10 MHz

A. COMPARISON EXPERIMENT WITH ISING MACHINE

In this subsection, we describe the experimental results of the proposed CIM-based, D-Wave-based, and ES-based RA in a small-scale UAV network with varying numbers of UAVs and channels. The purpose of this subsection is to compare the performance in the data rates of the D-Wave and CIM, which are both Ising machines. In the performance evaluation, the results of the D-Wave-based RA are achieved using the Advantage system 4.1, which is the quantum processing unit (QPU) of the D-Wave and capable of handling approximately 5000 qubits. The CIM used a machine capable of handling 2048 spins developed by Nippon Telegraph and Telephone (NTT). Table 3 shows the parameter settings of the small-scale UAV network in the performance evaluation, and Fig. 2 illustrates the placement of UAVs and GUs. The configuration of the small-scale network was set to a scale that D-Wave could realistically solve. Under these conditions, we obtained the results for the variation in the data rate with varying numbers of UAVs and channels, presented in Figs. 3 and 4, respectively.

TABLE 3. Parameter settings in a small-scale UAV network.

Parameter	Value
Number of GUs N	5
Number of UAVs M	4 (3,4,5)
Number of subchannels K	2 (1,2,3)
Transmission power P_l	100 mW

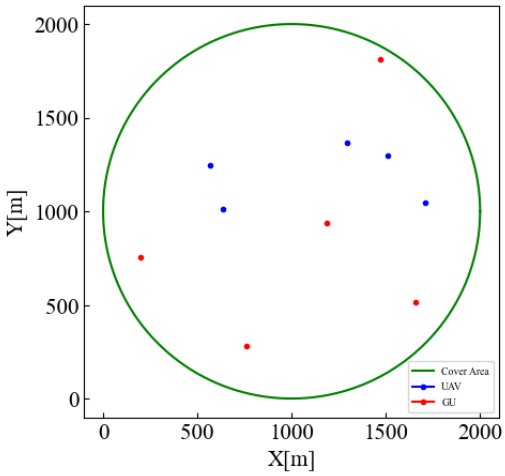

FIGURE 2. The placement of the UAVs and GUs in the small-scale UAV network.

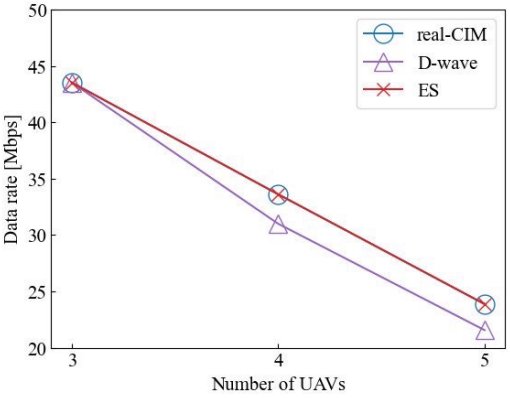

FIGURE 3. Total data rate in the small-scale UAV network with varying number of UAVs.

In Fig. 3, the results show the variation in the data rate when changing the number of UAVs from 3 to 5 while fixing the number of channels at 2. We introduced ES as a comparative method for obtaining the exact optimal solution. From Fig. 3, it can be observed that the proposed real-CIM consistently reaches the optimal solution, while D-Wave fails to reach the optimal data rate as the number of UAVs increases. The performance difference between CIM and D-Wave is attributed to the different representations of spins, and it is known that the performance of D-Wave degrades as the scale increases [30]. Therefore, the increase in the number of UAVs and the size of the UAV network likely led to a deterioration in performance for the D-Wave-based RA method. Moreover, the data rate decreases for all methods as the number of UAVs increases. The reason is that the increase in the number of UAVs causes stronger interference between channels when the number of channels is fixed.

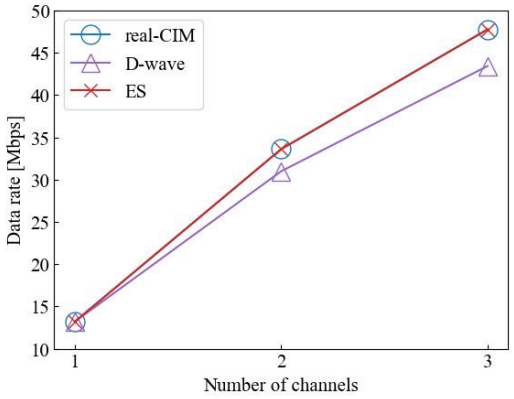

FIGURE 4. Total data rate in the small-scale UAV network with varying number of channels.

Fig. 4 shows the results of variation in the data rate when fixing the number of UAVs at 4 and changing the number of channels from 1 to 3. From Fig. 4, it can be observed that the proposed real-CIM consistently reaches the optimal solution, while D-Wave fails to reach the optimal data rate as the number of channels increases. The reason is similar to that of Fig. 3, as the performance of D-Wave deteriorates with an increase in the size of the UAV network. Moreover, the data rate increases for all methods as the number of channels increases. This reason is that the increase in the number of channels while keeping the number of UAVs fixed, reduces the impact of inter-channel interference.

B. PERFORMANCE EVALUATION IN A MIDDLE-SCALE UAV NETWORK

In this subsection, we describe the simulation results in a middle-scale UAV network. The purpose of this evaluation is to confirm that the proposed method can achieve optimal solutions. To compare with the optimal solution obtained by ES, the configuration of the middle-scale network was set to a scale that ES could solve within a realistic time. We introduce ES as a comparative method for obtaining the exact optimal solution. We also compare two heuristic algorithms, i.e., SA and SD. The number of iterations of CIM and SA is set to 500. Table 4 shows the simulation parameters related to the UAV network, and Fig. 5 illustrates the placement of UAVs and GUs in the UAV network. Under these conditions, we obtained the results for the variation in the data rate with varying numbers of UAVs and the channels, presented in Figs. 6 and 7, respectively.

TABLE 4. Parameter settings in a middle-scale UAV network.

Parameter	Value
Number of ground users N	8
Number of UAVs M	5 (3,4,5)
Number of subchannels K	2 (2,3,4)
Transmission power P_l	100 $\sim$ 1000 mW

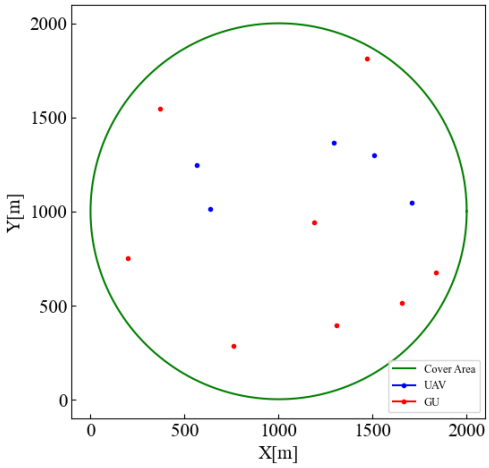

FIGURE 5. UAVs and GUs placement in the middle-scale UAV network.

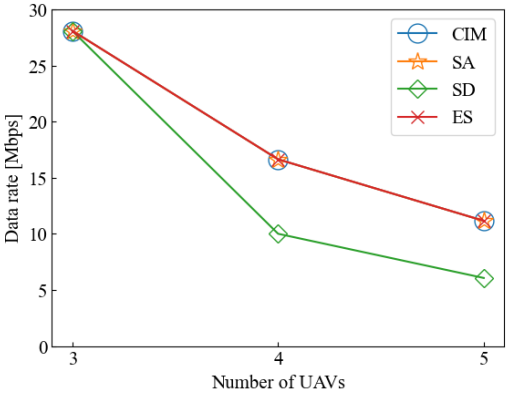

FIGURE 6. Total data rate in the middle-scale UAV network with varying numbers of UAVs.

In Fig. 6, the results show the variation in the data rate when changing the number of UAVs from 3 to 5 while fixing the number of channels at 2. From Fig. 6, it can be observed that the CIM and SA consistently reach the optimal solution, while SD fails to reach the optimal data rate as the number of UAVs increases. This is because SD is a simple algorithm for searching for the optimal solution, operating quickly but prone to getting stuck in the local minimum. Therefore, as the scale of the UAV network increased, it was difficult for SD to

reach the optimal solution. Moreover, it also shows a decrease in the data rate as the number of UAVs increases. The reason is the same as that in Fig. 3, i.e., the inference in the number of UAVs increases.

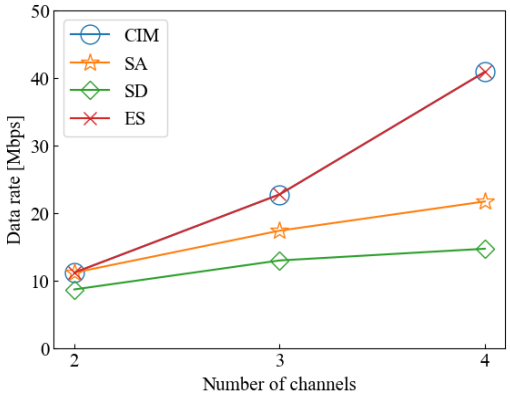

FIGURE 7. Total data rate in the middle-scale UAV network with varying numbers of channels.

In Fig. 7, the results show the variation in the data rate when fixing the number of UAVs at 5 and changing the number of channels from 2 to 4. From the Fig., it can be observed that the CIM consistently reaches the optimal solution, while SA and SD fail to reach the optimal data rate as the number of channels increases. SA consistently reached the exact optimal solution in Fig. 6; however, in Fig. 7, it is observed that SA fails to reach the exact optimal solution as the scale increases. This is attributed to the larger scale of the UAV network in Fig. 7 and the number of iterations. SA is an algorithm that may reach the exact optimal solution by increasing the number of iterations. However, within the same iterations as the CIM, i.e., 500 iterations, the SA could not achieve the exact optimal solution while CIM can, which shows that the CIM method can achieve higher performance under the same iterations and settings. To reach the exact optimal solution using SA, it is necessary to increase the program execution time and the iteration number beyond 500. Regarding the SD, the reason that it could not achieve the optimal solution is the same as that in Fig. 6, i.e., getting stuck in the local minimum. Moreover, for the same reason in Fig. 4, the results show an increase in the data rate as the number of channels increases.

C. PERFORMANCE EVALUATION IN A LARGE-SCALE UAV NETWORK

In this subsection, we describe the simulation results in a large-scale UAV network. The purpose of this evaluation is to assess the performance of the proposed CIM-based RA method and compare it to other heuristic algorithms to verify the superiority of the proposed method in the data rate and processing time. Since the performance is evaluated in a large-scale UAV network, ES cannot be executed in a realistic time frame and is therefore not included in the comparative methods. To keep the execution time the same, we set the number of iterations for CIM and SA to 1000. Table 5 shows the parameters used in the large-scale UAV network, and Fig. 8 illustrates the placement of UAVs and GUs. Under these conditions, we obtained the results for the variation in the data rate by changing the numbers of UAVs and channels, presented in Figs. 9 and 10, respectively. In addition, Fig. 11 shows the results for the computation time for each method.

TABLE 5. Parameter settings in a large-scale UAV network.

Parameter	Value
Number of ground users N	40
Number of UAVs M	13 (11,12,13,14,15)
Number of subchannels K	10 (8,9,10,11,12)
Transmission power P_l	$1 \sim 10$ W

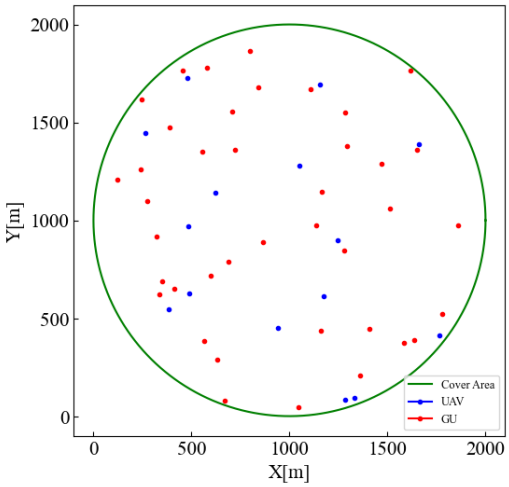

FIGURE 8. UAVs and GUs placement in the large-scale UAV Network.

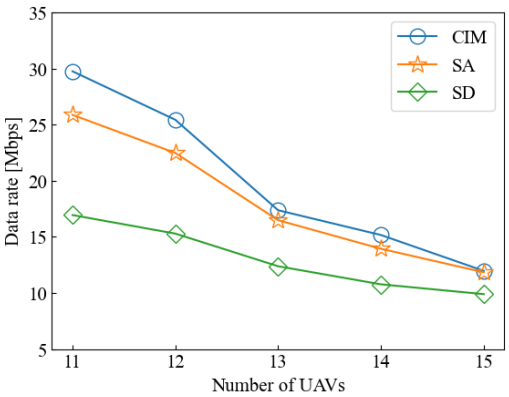

FIGURE 9. Total data rate for the varying number of UAVs in the large-scale UAV network.

In Fig. 9, the result shows the variation in the data rate when changing the number of UAVs from 11 to 15 while fixing the number of channels at 10. From these results, it is observed that the proposed CIM-based method achieved the highest data rate compared to other methods, especially when the number of UAVs is 11, which is evident that the CIM outperforms other comparison methods. This can be attributed to the environment with 10 available channels, where the impact of channel interference on network performance due to RA is substantial. Conversely, in the case of 15 UAVs, increased channel interference results in degraded network

performance. Regardless of how RA is conducted, there is no significant difference in network performance. Hence, the performance gap among the methods is considered small. Moreover, it shows a decrease in the data rate as the number of UAVs increases for the same reason as that in Figs. 3 and 6.

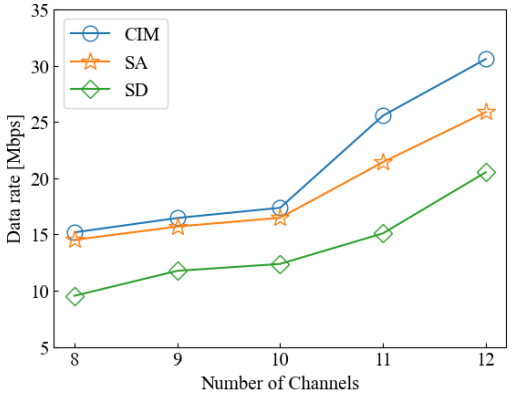

FIGURE 10. Total data rate for the varying number of channels in the large-scale UAV network.

In Fig. 10, the result shows the variation in the data rate when fixing the number of UAVs at 13 and changing the number of channels from 8 to 12. It is observed that the proposed CIM-based method achieved the highest data rate compared to other methods, especially for 12 channels. This can be attributed to the environment with 13 available UAVs, where the impact of channel interference on network performance due to RA is substantial. Moreover, it shows an increase in the data rate as the number of channels increases. The reason is the same as that in Figs. 4 and 7. In summary, from Figs. 9 and 10, it can be observed that when the interference of the UAV network is small, the CIM solution significantly outperforms other comparison methods.

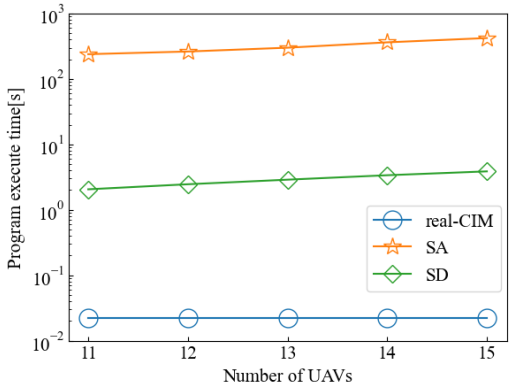

FIGURE 11. Computational time for the varying number of UAVs in the large-scale UAV network.

Fig. 11 shows the program execution time when the number of channels is fixed at 10 and the number of UAVs is changed from 11 to 15, following the same pattern as Fig. 9. SA and SD were evaluated in terms of program execution time using a computer with with Intel(R) Xeon(R) Gold 5222 CPU (3.80GHz). It can be observed that the execution time follows the order of real-CIM, SD, and SA in terms of speed. Combining the results of Fig. 9 and 11, it can be concluded that SD operates quicker but with bad performance, SA is slower but exhibits good performance, and CIM operates at ultra-fast speed with excellent performance when using a real Ising machine. Notably, the execution time for CIM is based on the use of the real CIM. In previous research, CIM can solve problems of up to 100,000 spins in 22 ms [28]. Moreover, D-Wave currently has a commercially available qubit count of approximately 5000 qubits. Since the scale of the large-scale UAV network is about 12,000 spins, which could not be implemented in D-Wave, D-Wave could not be included as a comparative method in this setting.

VII. DISCUSSION

In this section, we discuss the findings obtained in this study.

- First, we conducted comparative experiments using the real-CIM and D-wave, which are real Ising machines. Since D-wave is only capable of solving small-scale problems due to difficulties in handling large-scale problems internally, we evaluated its performance in total data rate in a small-scale UAV network. The results showed that our proposed real-CIM method can achieve a higher total data rate compared to D-Wave with varying numbers of UAVs and channels, especially when the scale of the UAV network increases. Moreover, the real-CIM-based method can achieve the optimal total data rate as the ES-based method. This aligns with the results obtained in previous studies on a different optimization problem [30].
- Next, we performed simulation comparisons between CIM and other heuristic algorithms, i.e., SA-based and SD-based methods and ES-based methods in a middle-scale UAV network with varying numbers of UAVs and channels. The middle-scale scale is the limit at which an ES can be realistically simulated in a reasonable amount of time. The results demonstrate that the proposed CIM-based method outperforms other heuristic algorithms in terms of the data rate and can achieve the optimal solutions as the ES method. Previous studies conducted simulation evaluations at this scale [14]. However, it is difficult to consider this scale realistic as the number of users is particularly low. Therefore, we conducted evaluations on a larger-scale UAV network.
- Then, we conducted simulation comparisons between CIM and other heuristic algorithms, i.e., SA-based and SD-based methods, in a large-scale UAV network with varying numbers of UAVs and channels. The results show that CIM exhibits a higher data rate performance compared to the heuristic algorithms. Moreover, since the ES may cost a large amount of time to achieve the optimal solutions in such a large-scale UAV network, it is difficult to be used for the RA problem in this scenario.

- Finally, the comparison of the computation time between the real-CIM and the heuristic algorithms is conducted in a large-scale UAV network. SA and SD represent the simulation execution time on a general CPU, while for CIM, we cited previous research [28] that solved a 100,000-spin problem in 22ms. Since the number of spins that needs to be used in the large-scale UAV network considered in this study is a maximum of 12,000 spins, we consider it realistically feasible to solve it in at least 22ms. As for D-wave, it currently has approximately 5000 available qubits for commercial use, making it unable to solve problems of this scale. Therefore, a comparison of execution times with D-wave could not be made in this study. In previous studies [14], [15], methods using DRL have been widely proposed. While DRL is suitable for solving resource allocation problems in large-scale UAV networks, it requires large time for training or pre-training the learning model. Furthermore, there is a possibility of retraining when the configuration of the UAV network changes. Additionally, when operating the learned model in a real environment, it is desirable to have at least a millisecond order of processing time, but currently, it is in the order of seconds [14]. Considering these factors, we believe that our proposed CIM-based method is much more suitable than the DRL-based methods for addressing the RA optimization problem in large-scale UAV networks in the future.

In conclusion, the contribution of this study is the proposal of a method for rapidly performing complex wireless resource allocation in large-scale UAV networks, which has not been addressed in previous research. Additionally, we carefully conducted performance comparisons with a real Ising machine, D-Wave, ES algorithm, and other heuristic algorithms, demonstrating the effectiveness of the proposed method in the data rate and computational time.

VIII. CONCLUSION

This study investigates a fast UAV-user association, sub-channel assignment, and power control strategy to enhance communication efficiency in the presence of co-channel interference for large-scale UAV-aided wireless networks. We formulate and transform the problem into a QUBO problem to maximize the network SIR in UAV networks. Furthermore, we conduct performance evaluation between the proposed method, CIM, and other Ising machines or heuristic algorithms, targeting UAV networks of various scales. The effectiveness of the proposed method is demonstrated, revealing its advantages in handling larger-scale problems compared to other Ising machines and solving them faster than other heuristic algorithms.

REFERENCES

[1] Z. Ullah, F. Al-Turjman, and L. Mostarda, "Cognition in UAV-aided 5G and beyond communications: A survey," *IEEE Trans. Cognit. Commun. Netw.*, vol. 6, no. 3, pp. 872–891, Sep. 2020.

[2] Y. Liu, J. Yan, and X. Zhao, "Deep reinforcement learning based latency minimization for mobile edge computing with virtualization in maritime UAV communication network," *IEEE Trans. Veh. Technol.*, vol. 71, no. 4, pp. 4225–4236, Apr. 2022.

[3] A. Ullah, W. Choi, Z. H. Abbas, and G. Abbas, "Aerial-terrestrial networks with multi-antenna transmissions: How many UAVs need to be deployed?" *IEEE Trans. Veh. Technol.*, vol. 73, no. 2, pp. 2212–2226, Feb. 2024.

[4] O. Sami Oubbati, M. Atiquzzaman, T. A. Ahanger, and A. Ibrahim, "Softwarization of UAV networks: A survey of applications and future trends," *IEEE Access*, vol. 8, pp. 98073–98125, 2020.

[5] M. Mozaffari, W. Saad, M. Bennis, Y.-H. Nam, and M. Debbah, "A tutorial on UAVs for wireless networks: Applications, challenges, and open problems," *IEEE Commun. Surveys Tuts.*, vol. 21, no. 3, pp. 2334–2360, 3rd Quart., 2019.

[6] Q. V. Do, Q.-V. Pham, and W.-J. Hwang, "Deep reinforcement learning for energy-efficient federated learning in UAV-enabled wireless powered networks," *IEEE Commun. Lett.*, vol. 26, no. 1, pp. 99–103, Jan. 2022.

[7] Y. Zeng, R. Zhang, and T. J. Lim, "Throughput maximization for UAV-enabled mobile relaying systems," *IEEE Trans. Commun.*, vol. 64, no. 12, pp. 4983–4996, Dec. 2016.

[8] S. Zhang, H. Zhang, B. Di, and L. Song, "Cellular UAV-to-X communications: Design and optimization for multi-UAV networks," *IEEE Trans. Wireless Commun.*, vol. 18, no. 2, pp. 1346–1359, Feb. 2019.

[9] P. Yang, X. Cao, X. Xi, Z. Xiao, and D. Wu, "Three-dimensional drone-cell deployment for congestion mitigation in cellular networks," *IEEE Trans. Veh. Technol.*, vol. 67, no. 10, pp. 9867–9881, Oct. 2018.

[10] B. Shang, V. Marojevic, Y. Yi, A. S. Abdalla, and L. Liu, "Spectrum sharing for UAV communications: Spatial spectrum sensing and open issues," *IEEE Veh. Technol. Mag.*, vol. 15, no. 2, pp. 104–112, Jun. 2020.

[11] L. Wang, H. Yang, J. Long, K. Wu, and J. Chen, "Enabling ultra-dense UAV-aided network with overlapped spectrum sharing: Potential and approaches," *IEEE Netw.*, vol. 32, no. 5, pp. 85–91, Sep. 2018.

[12] C. Qiu, Z. Wei, Z. Feng, and P. Zhang, "Joint resource allocation, placement and user association of multiple UAV-mounted base stations with in-band wireless backhaul," *IEEE Wireless Commun. Lett.*, vol. 8, no. 6, pp. 1575–1578, Dec. 2019.

[13] M.-N. Nguyen, L. D. Nguyen, T. Q. Duong, and H. D. Tuan, "Real-time optimal resource allocation for embedded UAV communication systems," *IEEE Wireless Commun. Lett.*, vol. 8, no. 1, pp. 225–228, Feb. 2019.

[14] Q. Hou, Y. Cai, Q. Hu, M. Lee, and G. Yu, "Joint resource allocation and trajectory design for multi-UAV systems with moving users: Pointer network and unfolding," *IEEE Trans. Wireless Commun.*, vol. 22, no. 5, pp. 3310–3323, May 2023.

[15] Z. Chang, H. Deng, L. You, G. Min, S. Garg, and G. Kaddoum, "Trajectory design and resource allocation for multi-UAV networks: Deep reinforcement learning approaches," *IEEE Trans. Netw. Sci. Eng.*, vol. 10, no. 5, pp. 2940–2951, May 2023.

[16] *D-Wave System*. Accessed: Dec. 2023. [Online]. Available: https://www.dwavesys.com/

[17] H. Takesue, K. Inaba, T. Inagaki, T. Ikuta, Y. Yamada, T. Honjo, T. Kazama, K. Enbutsu, T. Umeki, and R. Kasahara, "Simulating Ising spins in external magnetic fields with a network of degenerate optical parametric oscillators," *Phys. Rev. Appl.*, vol. 13, no. 5, pp. 54–59, May 2020.

[18] D. Yang, Q. Wu, Y. Zeng, and R. Zhang, "Energy tradeoff in ground-to-UAV communication via trajectory design," *IEEE Trans. Veh. Technol.*, vol. 67, no. 7, pp. 6721–6726, Jul. 2018.

[19] H. Wang, J. Wang, G. Ding, L. Wang, T. A. Tsiftsis, and P. K. Sharma, "Resource allocation for energy harvesting-powered D2D communication underlaying UAV-assisted networks," *IEEE Trans. Green Commun. Netw.*, vol. 2, no. 1, pp. 14–24, Mar. 2018.

[20] J. Lee and V. Friderikos, "Interference-aware path planning optimization for multiple UAVs in beyond 5G networks," *J. Commun. Netw.*, vol. 24, no. 2, pp. 125–138, Apr. 2022.

[21] Z. Li, M. Chen, C. Pan, N. Huang, Z. Yang, and A. Nallanathan, "Joint trajectory and communication design for secure UAV networks," *IEEE Commun. Lett.*, vol. 23, no. 4, pp. 636–639, Apr. 2019.

[22] Y. Guo, S. Yin, and J. Hao, "Joint placement and resources optimization for multi-user UAV-relaying systems with underlaid cellular networks," *IEEE Trans. Veh. Technol.*, vol. 69, no. 10, pp. 12374–12377, Oct. 2020.

[23] Y. Zhou, C. Pan, P. L. Yeoh, K. Wang, M. Elkashlan, B. Vucetic, and Y. Li, "Secure communications for UAV-enabled mobile edge computing systems," *IEEE Trans. Commun.*, vol. 68, no. 1, pp. 376–388, Jan. 2020.

[24] K. Wu, X. Cao, P. Yang, Z. Yu, D. O. Wu, and T. Q. S. Quek, "QoE-driven video transmission: Energy-efficient multi-UAV network optimization," *IEEE Trans. Netw. Sci. Eng.*, vol. 11, no. 1, pp. 366–379, Jan. 2024.
[25] Z. Han, T. Zhou, T. Xu, and H. Hu, "Joint user association and deployment optimization for delay-minimized UAV-aided MEC networks," *IEEE Wireless Commun. Lett.*, vol. 12, no. 10, pp. 1791–1795, Oct. 2023.
[26] P. L. Mcmahon, A. Marandi, Y. Haribara, R. Hamerly, C. Langrock, S. Tamate, T. Inagaki, H. Takesue, S. Utsunomiya, K. Aihara, R. L. Byer, M. M. Fejer, H. Mabuchi, and Y. Yamamoto, "A fully programmable 100-spin coherent Ising machine with all-to-all connections," *Science*, vol. 354, no. 6312, pp. 614–617, Nov. 2016.
[27] T. Inagaki, Y. Haribara, K. Igarashi, T. Sonobe, S. Tamate, T. Honjo, A. Marandi, P. L. Mcmahon, T. Umeki, K. Enbutsu, O. Tadanaga, H. Takenouchi, K. Aihara, K.-I. Kawarabayashi, K. Inoue, S. Utsunomiya, and H. Takesue, "A coherent Ising machine for 2000-node optimization problems," *Science*, vol. 354, no. 6312, pp. 603–606, Nov. 2016.
[28] T. Honjo, T. Sonobe, K. Inaba, T. Inagaki, T. Ikuta, Y. Yamada, T. Kazama, K. Enbutsu, T. Umeki, R. Kasahara, K.-I. Kawarabayashi, and H. Takesue, "100,000-spin coherent Ising machine," *Sci. Adv.*, vol. 7, no. 40, pp. 1–10, Oct. 2021.
[29] A. Lucas, "Ising formulations of many NP problems," *Frontiers Phys.*, vol. 2, no. 40, p. 5, 2014.
[30] R. Hamerly et al., "Experimental investigation of performance differences between coherent Ising machines and a quantum annealer," *Sci. Adv.*, vol. 5, no. 5, May 2019, Art. no. eaau0823.
[31] T. Ohyama, Y. Kawamoto, and N. Kato, "Intelligent reflecting surface (IRS) allocation scheduling method using combinatorial optimization by quantum computing," *IEEE Trans. Emerg. Topics Comput.*, vol. 10, no. 3, pp. 1633–1644, Jul. 2022.
[32] T. Otsuka, A. Li, H. Takesue, K. Inaba, K. Aihara, and M. Hasegawa, "High-speed resource allocation algorithm using a coherent Ising machine for NOMA systems," *IEEE Trans. Veh. Technol.*, vol. 73, no. 1, pp. 707–723, Jan. 2024.
[33] T. Otsuka, K. Kurasawa, Z. Duan, A. Li, K. Sato, H. Takesue, K. Aihara, K. Inaba, and M. Hasegawa, "Coherent Ising machine based optimal channel allocation and user pairing in NOMA networks," in *Proc. Int. Conf. Artif. Intell. Inf. Commun. (ICAIIC)*, Apr. 2021, pp. 1–4.
[34] K. Kurasawa, K. Hashimoto, A. Li, K. Sato, K. Inaba, H. Takesue, K. Aihara, and M. Hasegawa, "A high-speed channel assignment algorithm for dense IEEE 802.11 systems via coherent Ising machine," *IEEE Wireless Commun. Lett.*, vol. 10, no. 8, pp. 1682–1686, Aug. 2021.
[35] H. Ito, Y. Jiang, H. Yasuda, H. Takesue, K. Aihara, and M. Hasegawa, "High-speed optimization method for resource allocation in wireless communication systems by coherent Ising machine," in *Proc. Int. Conf. Artif. Intell. Inf. Commun. (ICAIIC)*, Feb. 2020, pp. 093–097.
[36] N. Babu, C. B. Papadias, and P. Popovski, "Energy-efficient 3-D deployment of aerial access points in a UAV communication system," *IEEE Commun. Lett.*, vol. 24, no. 12, pp. 2883–2887, Dec. 2020.
[37] A. Al-Hourani, S. Kandeepan, and S. Lardner, "Optimal LAP altitude for maximum coverage," *IEEE Wireless Commun. Lett.*, vol. 3, no. 6, pp. 569–572, Dec. 2014.
[38] S. Utsunomiya, K. Takata, and Y. Yamamoto, "Mapping of Ising models onto injection-locked laser systems," *Opt. Exp.*, vol. 19, no. 19, p. 18091, 2011.
[39] M. S. Hossain and M. A. Simaan, "Investigating the performance of steepest descent, Newton–Raphson, and Fletcher–Reeves approaches in unconstrained minimization problems," in *Proc. IEEE 13th Annu. Comput. Commun. Workshop Conf. (CCWC)*, Mar. 2023, pp. 61–68.
[40] E. Aarts and J. Korst, "Boltzmann machines for traveling salesman problems," *Eur. J. Oper. Res.*, vol. 39, pp. 79–95, Jan. 1989.

TSUKUMO FUJITA received the B.Eng. and M.Eng. degrees from the Department of Electrical Engineering, Faculty of Engineering, Tokyo University of Science, Tokyo, Japan, in 2022, and 2024, respectively. His research interests include UAV, quantum annealing, and coherent Ising machines. He is currently with Nomura Research Institute, Japan.

AOHAN LI (Member, IEEE) received the Ph.D. degree from Keio University, Yokohama, Japan, in 2020. From 2020 to 2022, she was an Assistant Professor with Tokyo University of Science, Tokyo, Japan, where she is currently a Visiting Researcher. She is also an Assistant Professor with The University of Electro-Communications, Tokyo. She has published over 80 peer-reviewed journals and international conference papers. Her current research interests include resource management, quantum annealing, machine learning, and the Internet of Things. She is a member of IEICE. She was a recipient of the Ninth International Conference on Communications and Networking in China 2014 (CHINACOM'14) Best Paper Award, the Third International Conference on Artificial Intelligence in Information and Communication (ICAIIC'21) Excellent Paper Award, and the Telecom System Technology Student Excellent Paper Award of the Telecommunications Advancement Foundation, Japan, in 2021.

QUANG VINH DO received the bachelor's degree in electrical engineering from Ho Chi Minh City University of Technology, Vietnam, in 2009, the master's degree in electronic and computer engineering from RMIT University, Australia, in 2013, and the Ph.D. degree in electrical engineering from the University of Ulsan, South Korea, in 2020. He was a Postdoctoral Researcher with the University of Ulsan, from September 2020 to February 2021. From March 2021 to August 2023, he was a Post-Doctoral Research Fellow with the Artificial Intelligence Research Center, Pusan National University, South Korea. He is currently a Lecturer at Ton Duc Thang University, Vietnam. His research interests include developing and applying artificial intelligence techniques to wireless communication networks.

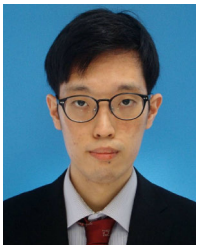

TEPPEI OTSUKA received the B.Eng. and M.Eng. degrees from the Department of Electrical Engineering, Faculty of Engineering, Tokyo University of Science, Tokyo, Japan, in 2021 and 2023, respectively. He is currently with NTT Docomo, Inc. Japan. His research interests include NOMA, quantum annealing, and coherent Ising machine.

SEON-GEUN JEONG received the B.S. degree in electrical engineering from Pusan National University, Busan, South Korea, in 2017, where he is currently pursuing the integrated Ph.D. degree with the Department of Information Convergence Engineering. His current research interests include wireless networks, quantum computing, quantum annealing, quantum machine learning, and quantum information.

WON-JOO HWANG (Senior Member, IEEE) received the B.S. and M.S. degrees in computer engineering from Pusan National University, Busan, South Korea, in 1998 and 2000, respectively, and the Ph.D. degree in information systems engineering from Osaka University, Osaka, Japan, in 2002. From 2002 to 2019, he was employed as a full-time Professor with Inje University, Gimhae, South Korea. He is currently a full-time Professor with the Biomedical Convergence Engineering Department, Pusan National University. His research interests include optimization theory, game theory, machine learning, and data science for wireless communications and networking.

HIROKI TAKESUE (Member, IEEE) received the B.Eng., M.Eng., and Ph.D. degrees in engineering science from Osaka University, Japan, in 1994, 1996, and 2002, respectively. He joined the NTT Laboratories, in 1996. Since then, he has been engaged in research on quantum communication and photonic computation. He is currently a Senior Distinguished Researcher with NTT and the Group Leader of Quantum Optical State Control Research Group, NTT Basic Research Laboratories.

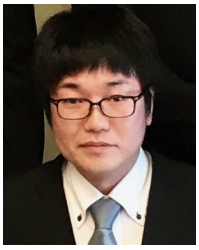

KENSUKE INABA received the B.E., M.E., and Dr.Eng. degrees from the Department of Applied Physics, Osaka University, in 2003, 2005, and 2007, respectively. He is currently a Senior Research Scientist with the Quantum Optical State Control Research Group, NTT Basic Research Laboratories, and he has been working for this laboratory, since 2008. Here, he has been theoretically studying many body systems and photonic computation.

KAZUYUKI AIHARA received the B.E. degree in electrical engineering and the Ph.D. degree in electronic engineering from The University of Tokyo, Japan, in 1977 and 1982, respectively. Currently, he is a University Professor and a Professor Emeritus with The University of Tokyo. His research interests include mathematical modeling of complex systems, parallel distributed processing with spatio-temporal neurodynamics, and time series analysis of complex data.

MIKIO HASEGAWA (Member, IEEE) received the B.Eng., M.Eng., and Dr.Eng. degrees from Tokyo University of Science, Japan, in 1995, 1997, and 2000, respectively. From 1997 to 2000, he was a Research Fellow with Japan Society for the Promotion of Science (JSPS). From 2000 to 2007, he was with the Communications Research Laboratory (CRL), Ministry of Posts and Telecommunications, which was reorganized as the National Institute of Information and Communications Technology (NICT), in 2004. Currently, he is a Professor with the Department of Electrical Engineering, Faculty of Engineering, Tokyo University of Science. His research interests include mobile networks, cognitive radio, neural networks, machine learning, and optimization techniques. He is a Senior Member of IEICE.